

Combined Super-Resolution Fluorescence and Coaxial 3-D Scanning Microwave Microscopy: Proof-of-Concept In-Liquid Live-Cell Imaging: Toward a Biological Nano-Radar

Chia-Hung Lee, Kamel Haddadi¹, *Member, IEEE*, and Peter J. Burke², *Fellow, IEEE*

Abstract—We present a proof-of-concept 3-D scanning microwave microscope based on a miniaturized coaxial probe combined with high-resolution fluorescence microscopy for in-liquid operation and live-cell imaging. The system simultaneously provides electric (GHz) and optical (super-resolution) imaging of live cells for broad applications in life sciences. It combines advantages offered by both open-ended coaxial probing and near-field scanning microwave microscopy (SMM) for accurate and quantitative local microwave measurements. The shielded tip minimizes unwanted absorption of microwaves by the biological media as compared to fringe fields of unshielded tips which we previously showed absorb over 90% of the signal and mask the true imaging signal. A proof-of-concept system built up with commercial off-the-shelf (COTS) components is demonstrated in the frequency range 0.01–6 GHz with micrometric spatial resolution, only limited by the coaxial probe geometry. Our work at the microscale lays the technological foundation for a true nano-radar in liquid cell imaging system that will come with further advances in nanofabrication technologies applied to coaxial probes and can be integrated with super-resolution optical microscopy, for an integrated full electromagnetic spectrum to probe biology at the nanoscale, from dc to lightwave.

Index Terms—Cell imaging, high-resolution fluorescence, near-field scanning microwave microscopy (SMM), open-ended coaxial probe.

I. INTRODUCTION

NEAR-FIELD scanning microwave microscopy (SMM) tools have pioneered many applications, notably

Received 25 April 2024; accepted 26 May 2024. This work was supported in part by NIH under Grant 1 R01 CA259635-01A1 and Grant 3 R01 CA243033-03S1A1; in part by the National Science Foundation (NSF) under Award 2153425; in part by the Army Research Office through ARO under Contract W911NF-18-1-0076, Contract W911NF2010103, and Contract W911NF1910369; in part by Air Force Office of Scientific Research (AFOSR) under Grant FA9550-23-1-0061; in part by the Air Force Office of Scientific Research under Award FA9550-23-1-0436 and Award FA9550-23-1-0061. (Corresponding author: Peter J. Burke.)

Chia-Hung Lee is with the Department of Biomedical Engineering, University of California at Irvine, Irvine, CA 92697 USA (e-mail: chiahu4@uci.edu).

Peter J. Burke is with the Department of Biomedical Engineering and the Department of Electrical and Engineering and Computer Science, University of California at Irvine, Irvine, CA 92697 USA (e-mail: pburke@uci.edu).

Kamel Haddadi is with the CNRS, Université Polytechnique Hauts-de-France, UMR 8520-IEMN-Institut d'Électronique de Microélectronique et de Nanotechnologie, USR 3380-IRCICA, University of Lille, 59000 Lille, France (e-mail: kamel.haddadi@ieec.org).

Color versions of one or more figures in this letter are available at <https://doi.org/10.1109/LMWT.2024.3483071>.

Digital Object Identifier 10.1109/LMWT.2024.3483071

including mapping of the electromagnetic properties of materials at the nanoscale [1], [2], [3], [4], [5], [6], [7]. The fringe fields from the scanning sharp metal tip typically used can be a challenge, spreading the RF field far away from the tip and compromising the resolution. While Stanford approached this with a rectilinear MEMS process to shield the tip [8], a coaxial geometry is much simpler to model and manufacture, as demonstrated by Steinhauer et al. [9] and Vlahacos et al. [10].

SMM has been recently used to characterize biological cells [11], [12], [13], [14], [15], [16]. We demonstrated for the first time nanoscale imaging of vital isolated mitochondria at 7 GHz [15]. Recently, we took a major step forward by combining fluorescence and microwave microscopy to assay cell vitality characterized by physiological buffer [16]. Fringe fields of unshielded metal probes commonly found in planar cantilever type cause reduced imaging resolution and field distribution far from the tip, which is especially challenging in highly conductive NaCl liquid environments germane to the life sciences, where the liquid absorption of the fringe fields can cause 10 dB reduction in signal from the tip, as we showed in [16]. This was not considered in any previously shielded SMM measurements, such as Stanford's rectilinear geometry or Anlage's coaxial geometry, because none of those works addressed operation in a liquid environment. In this work, by exploiting the shielding demonstrated by Steinhauer et al. [9] and Vlahacos et al. [10], we demonstrate a shielded probe that can image live cells with a full XYZ scanning range compatible with simultaneous super-resolution fluorescence microscopy. Whereas in conventional SMM, the tip has to be right above the cell, the proposed approach is an advance in SMM since we have a Z-axis, given the unique opportunity to image above and inside the cell.

Thus, the major advance of this article is a proof of concept combining in one system the ingredients previously developed independently: 1) coax (shielded) tips; 2) 3-D XYZ scanning; 3) liquid operation; 4) live-cell interrogation; and 5) integration with fluorescence microscopy.

II. EXPERIMENTAL COAX-SMM

Fig. 1 shows the key components of our system. The miniaturized coaxial probe consists of an open-ended 50 Ω semi-rigid cable (PASTERNAK¹ PE-020SR with inner conductor copper clad steel $\varnothing = 100 \mu\text{m}$, dielectric polytetrafluoroethylene (PTFE) $\varnothing = 384 \mu\text{m}$, and outer conductor

¹Registered trademark.

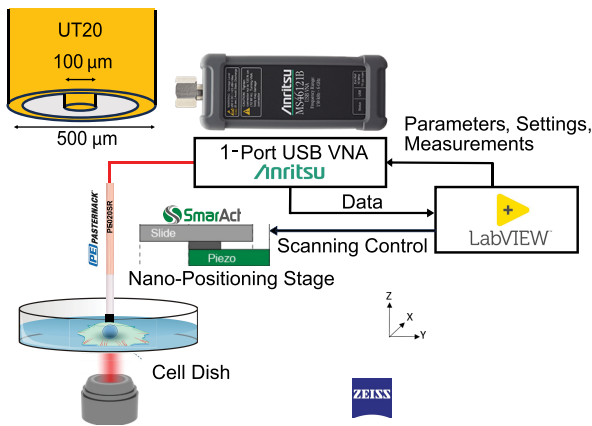


Fig. 1. System implementation of the proof-of-concept combined high-resolution fluorescence and coaxial 3-D SMM.

copper $\varnothing = 510 \mu\text{m}$) mounted on a coaxial SMA transition. This is the smallest commercial off-the-shelf (COTS) semi-rigid coax available and requires no fabrication other than cutting the end with a sharp razor blade. Commercial coax assemblies with an SMA connector already soldered on are readily available for modest cost.

The probe is connected through a series of rigid and flexible coaxial cables to a PC-controlled, 1-port USB ANRITSU¹ MS46121B vector network analyzer (VNA) with a frequency range of 150 kHz to 6 GHz. The rigid cable supporting the probe is attached to a scanning stage composed of three piezo-driven linear actuators from SMARACT¹ GmbH with scanning ranges of 16 mm in X - and Y -directions and 21 mm in Z -direction. The movements of the probe are controlled in close-loop operation with nanometer resolution and ± 40 nm repeatability (manufacturer data). The use of 3-D scanner technology is different from prior SMM work, in which 2-D scanners are used with only a coarse control in the z -direction. While it limits the XY resolution compared to 2-D scanners in dry environments, we found the liquid environment degraded the resolution even of pristine 2-D scanners to about 100 nm for unknown reasons [16]. Therefore, in moving from 2-D to 3-D, no resolution is lost for imaging in live-cell applications.

Existing SMM systems are able to position the tip in the z -direction, but not closed loop with 30 nm precision. That is what is new about the positioning system used here as opposed to all prior SMM systems, which primarily are designed to scan in XY and Z is only for coarse approach (not for scanning).

The probe is positioned and moved over the sample according to different microwave scanning modes (1-to-3-D) developed under LabVIEW. The fixed delivered input RF power is 3 dBm up to 4 GHz, -5 dBm in the range 4–6 GHz.

Role of fluorescence microscopy: The entire system is integrated on top of a super-resolution Airyscan confocal microscope in an integrated environmental chamber with temperature and CO_2 control. This is a proof of concept work showing a compatible system. For more extensive super-resolution cellular imaging on this exact same microscope, see our recent work [17].

III. SYSTEM CHARACTERIZATION (DRY)

The performance of the measurement system was experimentally evaluated by considering in-depth Z -scanning and lateral X/Y scanning modes. The probe has been preliminary

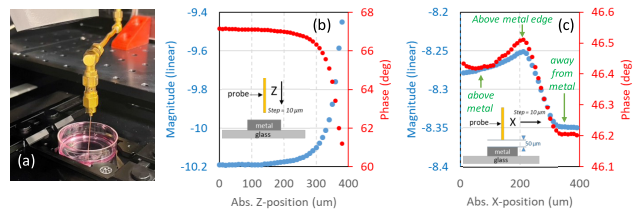


Fig. 2. Experimental study of the depth/lateral resolution ($f \sim 4$ GHz; IFBW = 10 Hz). (a) Photograph of the miniaturized open-ended coaxial probe above the MUT (MUT = Copper sheet $1 \times 1 \text{ mm}^2$). (b) Measured magnitude and phase of S_{11} as a function of the absolute Z -position. (c) Measured magnitude and phase of the S_{11} as a function of the absolute X -position.

characterized in free-space conditions to check that the complex reflection coefficient S_{11} is close to 1 with amplitude decreasing with frequency and phase with linear variation with frequency. We noticed some depth resonances at higher frequencies inherent to wave recombination in the microwave path. When the probe is close to a material sample, S_{11} changes as a function of both material properties and stand-off displacement. The material under test (MUT) consists of a copper sheet ($1 \times 1 \text{ mm}^2$, thickness = $100 \mu\text{m}$) positioned in the center of a cylindrical glass Petri dish (thickness = $160 \mu\text{m}$).

First, we studied the displacement dependence of the magnitude and phase shift of S_{11} in continuous wave (CW) operation at 4 GHz (freq. of $|S_{11}|$ with the load impedance near 50Ω). In this configuration, the intermediate frequency bandwidth (IFBW) was set to 10 Hz, and a mean of ten measurement points was considered for each Z -position to ensure high measurement accuracy. The probe is moved from an arbitrary position to the probe contact with an increment of $d_{\text{STEP}} = 10 \mu\text{m}$ [Fig. 1(a)]. For example, calculated standard deviations for the first scan position are 4.2×10^{-5} and $6.5^\circ \times 10^{-3}$ for the magnitude and phase shift of S_{11} respectively. Fig. 2(b) shows that the inner conductor diameter ($\varnothing = 100 \mu\text{m}$) governs the displacement at which microwaves penetrate from the probe aperture (high microwave sensitivity for absolute position in the range 300–400 μm). In a second step, considering the same measurement configuration, a linear scan (along the X -axis) of the MUT is performed at a stand-off set to $50 \mu\text{m}$ [Fig. 2(b)]. Both measured magnitude and phase are sensitive to the material properties. From these data, the most intense fields are generated near the inner conductor, as the resolution at the interface metal air is estimated to be $100 \mu\text{m}$ for a stand-off displacement of $50 \mu\text{m}$. The spatial extent of the microwave field sets a lower limit on the lateral spatial resolution (not investigated here), rather than the wavelength. These results are instructive as they suggest possible transposition of the method at the nanoscale by considering the future development of nano-coaxial probe structure. In this case, only the probe can be changed as the scanning stage has been thought and developed for future microwave imaging at the nanoscale.

IV. IN-LIQUID RF PROBING OF VITAL CELLS

A. Cells Preparation

HeLa cells were purchased from ATCC¹. HeLa (ATCC CCL-2) are epithelial adherent cell lines derived from cervical cancer cells with a diameter size in the range of 30–50 μm . The cells were cultured for 2–3 days in 75 cm^2 tissue flasks at 37°C and 5% CO_2 . The protease trypsin was used to detach

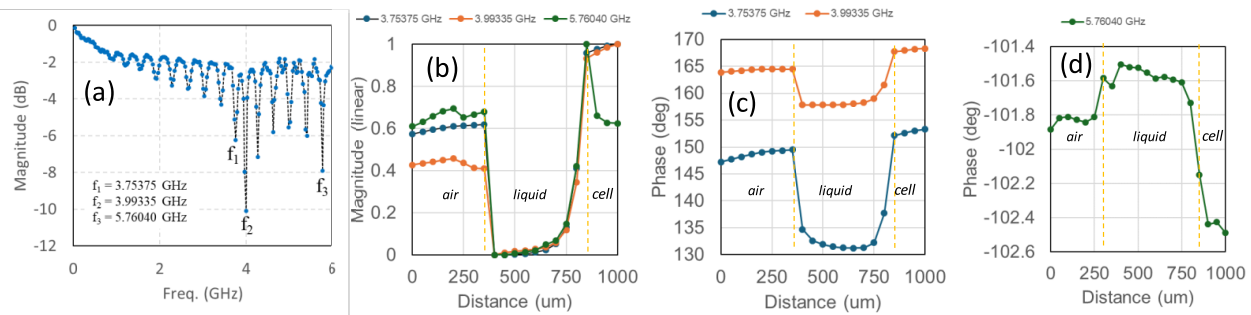


Fig. 3. (a) Broadband measurement above a metallic plate at a stand-off set to $80 \mu\text{m}$. (b) Measured complex reflection coefficient S_{11} as a function of the absolute Z-position for test frequencies 3.75375, 3.99335, and 5.76040 GHz (MUT = Hela [ATCC CCL-2] cells in physiological buffer, ZSTEP = $50 \mu\text{m}$). IFBW = 100 Hz.

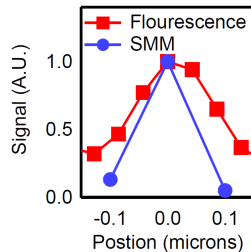


Fig. 4. Fluorescence intensity (red) and SMM signal (dPhase/dx) (blue). The full width at half max in both cases is about 100 nm.

cells from the flask and seeded at CELLview 4-compartment glass-bottom tissue culture dishes (Greiner Bio-One, 627 870), PS, 35/10 mm. After 12–24 h of incubation, the cells are tagged with TMRE potentiometric fluorescent dye (ex/em 549/574 nm) at 10 nM for live analysis and localization. A Zeiss¹LSM900 (w/incubation chamber, set to 37°C) with Airyscan¹ with an alpha Plan-Apochromat $63\times/1.4$ Oil DIC M27 objective is used to image the location of the cell and tip.

B. Microwave Cell Probing in Physiological Buffer

Broadband (0.01–6 GHz, step = 29.95 MHz) in-depth microwave probing was performed on live Hela cells. The coaxial probe starts approaching from the air and into the culture medium with an increment of $Z_{\text{STEP}} = 50 \mu\text{m}$ and a scan length of 1 mm. Based on a preliminary broadband measurement above a metallic plate at a stand-off set to $80 \mu\text{m}$, we select three test frequencies with the load impedance near 50Ω in the air [Fig. 3(a)]. Then, we show recorded data (raw, uncalibrated) with S_{11} contrasts between interfaces air–liquid and liquid–cell clearly distinguished [Fig. 3(b)–(d)].

Calibration at the probe aperture (beyond the scope of this study) can be used to quantify the local electromagnetic properties in the vicinity of the probe. When the probe approaches the liquid surface (displacement from 0 to $400 \mu\text{m}$), S_{11} variation is related to probe-to-liquid coupling. When the probe touched the liquid surface, abrupt shifts of both magnitude and phase of S_{11} were noticed with values depending on the dielectric constant and loss tangent of the physiological buffer. The probe immersed in the liquid showed a nearly constant signal that changed as the probe approached the cell. From 400 to $800 \mu\text{m}$, the probe penetrates the liquid with a nearly constant signal that varies significantly when the cell is in the near zone ($100 \mu\text{m}$ from the probe aperture). At the contact liquid cell, a shift is noticed for both the magnitude and phase of S_{11} for all the cases considered. As the probe presents a load impedance near 50Ω even in the liquid, the microwave complex reflection in the medium is relatively sensitive. Again,

a clear S_{11} contrast is visible when the probe touched the cell. The magnitude $|S_{11}|$ falls to a low value around -30 dB . In the displacement range of $800\text{--}1000 \mu\text{m}$, the probe presses the cell and therefore affects its overall dielectric constant (function of the density). In the displacement range of $800\text{--}1000 \mu\text{m}$, the probe presses the cell, and therefore, affects its overall dielectric constant (function of the density). This displacement range was set prior to the experiment and the thickness of the adherent HeLa cell is around $20 \mu\text{m}$. Because the Z resolution of the coax (discussed in Section III) is determined by the coax geometry/diameter (in this case about $100 \mu\text{m}$), the tip responds to the cell before it touches the surface of the cells.

In order to provide more experimental data comparing the fluorescence to the SMM imaging techniques, in Fig. 4 (red), we present fluorescence data of a cell membrane on our system, demonstrating sub 100 nm optical resolution [17], much better than the SMM in our current system that uses a micro-coax (Fig. 1). In order to compare ultimate limits, SMM signal taken from an unshielded tip in a similar system [16] is plotted in Fig. 4 (blue) to show SMM resolution in live-cell liquid SMM with an unshielded tip. This experimental data show that smaller tips result in SMM imaging resolution approaching that of super-resolution optical microscopy. With a shielded, nanoscale tip, the resolution of the SMM should improve further.

V. CONCLUSION

We demonstrate proof of concept of the combination of high-resolution fluorescence and coaxial microwave μ -probing on live cells. The approach proposed: 1) removes stray signal absorption by the highly conducting liquid media used in life sciences applications commonly found on conventional SMM and 2) provides simultaneous imaging in high-resolution optical fluorescence microscopy, which can easily be extended to super-resolution microscopy such as Airyscan and stimulated emission depletion (STED) (in fact, the system used was an Airyscan system). This work lays the foundation for future work using nanofabrication to create improved tip resolution using coaxial geometries. In conclusion, this work extends conventional 2-D dry unshielded SMM into in-liquid 3-D shielded liquid imaging, opening the door toward an integrated full electromagnetic spectrum to probe biology at the nanoscale, from dc to lightwave: A biological nano-radar.

ACKNOWLEDGMENT

Any opinions, findings, and conclusions or recommendations expressed in this material are those of the author(s) and do not necessarily reflect the views of the United States Air Force.

REFERENCES

- [1] E. A. Ash and G. Nicholls, "Super-resolution aperture scanning microscope," *Nature*, vol. 237, no. 5357, pp. 510–512, Jun. 1972.
- [2] A. Imtiaz, T. M. Wallis, and P. Kabos, "Near-field scanning microwave microscopy: An emerging research tool for nanoscale metrology," *IEEE Microw. Mag.*, vol. 15, no. 1, pp. 52–64, Jan. 2014.
- [3] P. H. Siegel, "Microwaves are everywhere: 'SMM: Nano-microwaves,'" *IEEE J. Microw.*, vol. 1, no. 4, pp. 838–852, Oct. 2021.
- [4] K. Haddadi, D. Glay, and T. Lasri, "A 60 GHz scanning near-field microscope with high spatial resolution sub-surface imaging," *IEEE Microw. Wireless Compon. Lett.*, vol. 21, no. 11, pp. 625–627, Nov. 2011.
- [5] T. Dargent et al., "An interferometric scanning microwave microscope and calibration method for sub-fF microwave measurements," *Rev. Sci. Instrum.*, vol. 84, no. 12, Dec. 2013, Art. no. 123705, doi: [10.1063/1.4848995](https://doi.org/10.1063/1.4848995).
- [6] M. Azizi and R. R. Mansour, "Design and sensitivity improvement of CMOS-MEMS scanning microwave microscopes," *IEEE Trans. Microw. Theory Techn.*, vol. 65, no. 8, pp. 2749–2761, Aug. 2017.
- [7] A. Tselev, "Near-field microwave microscopy: Subsurface imaging for in situ characterization," *IEEE Microw. Mag.*, vol. 21, no. 10, pp. 72–86, Oct. 2020.
- [8] K. Lai, W. Kundhikanjana, M. A. Kelly, and Z.-X. Shen, "Nanoscale microwave microscopy using shielded cantilever probes," *Appl. Nanoscience*, vol. 1, no. 1, pp. 13–18, May 2011.
- [9] D. E. Steinhauer, C. P. Vlahacos, S. K. Dutta, F. C. Wellstood, and S. M. Anlage, "Surface resistance imaging with a scanning near-field microwave microscope," *Appl. Phys. Lett.*, vol. 71, no. 12, pp. 1736–1738, Sep. 1997.
- [10] C. P. Vlahacos, R. C. Black, S. M. Anlage, A. Amar, and F. C. Wellstood, "Near-field scanning microwave microscope with 100m resolution," *Appl. Phys. Lett.*, vol. 69, no. 21, pp. 3272–3274, 1996.
- [11] M. Farina, A. Di Donato, D. Mencarelli, G. Venanzoni, and A. Morini, "High resolution scanning microwave microscopy for applications in liquid environment," *IEEE Microw. Wireless Compon. Lett.*, vol. 22, no. 11, pp. 595–597, Nov. 2012, doi: [10.1109/LMWC.2012.2225607](https://doi.org/10.1109/LMWC.2012.2225607).
- [12] M. Farina et al., "Investigation of fullerene exposure of breast cancer cells by time-gated scanning microwave microscopy," *IEEE Trans. Microw. Theory Techn.*, vol. 64, no. 12, pp. 4823–4831, Dec. 2016.
- [13] X. Jin, M. Farina, X. Wang, G. Fabi, X. Cheng, and J. C. M. Hwang, "Quantitative scanning microwave microscopy of the evolution of a live biological cell in a physiological buffer," *IEEE Trans. Microw. Theory Techn.*, vol. 67, no. 12, pp. 5438–5445, Dec. 2019.
- [14] Y. Chen et al., "Application of near-field scanning microwave microscopy in liquid environment," *IEEE Access*, vol. 10, pp. 75720–75728, 2022.
- [15] J. Li, Z. Nernati, K. Haddadi, D. C. Wallace, and P. J. Burke, "Scanning microwave microscopy of vital mitochondria in respiration buffer," in *IEEE MTT-S Int. Microw. Symp. Dig.*, Jun. 2018, pp. 115–118.
- [16] D. Ren et al., "An ultra-high bandwidth nano-electronic interface to the interior of living cells with integrated fluorescence readout of metabolic activity," *Sci. Rep.*, vol. 10, no. 1, p. 10756, Jul. 2020.
- [17] C. Lee, D. C. Wallace, and P. J. Burke, "Super-resolution imaging of voltages in the interior of individual, vital mitochondria," *ACS Nano*, vol. 18, no. 2, pp. 1345–1356, Jan. 2024.